

August 2008

# Open optoelectrowetting droplet actuation

Han-Sheng Chuang

*Purdue University*, [hchuang@purdue.edu](mailto:hchuang@purdue.edu)

Aloke Kumar

*Purdue University*, [kumar31@purdue.edu](mailto:kumar31@purdue.edu)

Steven Wereley

*Birck Nanotechnology Center, Purdue University*, [wereley@purdue.edu](mailto:wereley@purdue.edu)

Follow this and additional works at: <http://docs.lib.purdue.edu/nanopub>

---

Chuang, Han-Sheng; Kumar, Alope; and Wereley, Steven, "Open optoelectrowetting droplet actuation" (2008). *Birck and NCN Publications*. Paper 128.

<http://docs.lib.purdue.edu/nanopub/128>

This document has been made available through Purdue e-Pubs, a service of the Purdue University Libraries. Please contact [epubs@purdue.edu](mailto:epubs@purdue.edu) for additional information.

## Open optoelectrowetting droplet actuation

Han-Sheng Chuang, Aloke Kumar, and Steven T. Wereley<sup>a)</sup>

*Birck Nanotechnology Center and School of Mechanical Engineering, Purdue University, West Lafayette, Indiana 47907, USA*

(Received 28 May 2008; accepted 24 July 2008; published online 14 August 2008)

We present experimental realization of an open optoelectrowetting (o-OEW) device for liquid droplet manipulations. The o-OEW device is realized by coplanar electrodes and a photoconductor. The local switching effect for electrowetting resulting from illumination is based on the tunable impedance of the photoconductor. Dynamic virtual electrodes are created using projected images, leading to free planar movements of droplets. Basic operations such as transporting and merging were demonstrated. Translational speed up to 3.6 mm/s was measured. Equivalent circuit analysis shows that the operational frequency for the current setup ranges from 100 to 800 Hz. © 2008 American Institute of Physics. [DOI: 10.1063/1.2970047]

Digital microfluidics has been emerging as a promising development in lab-on-a-chip (LoC) systems.<sup>1–5</sup> A variety of droplet actuation methods have been conducted including thermal Marangoni effect,<sup>6</sup> photosensitive surface treatment,<sup>7</sup> surface acoustic wave,<sup>8</sup> liquid dielectrophoresis,<sup>9</sup> and electrowetting.<sup>1,10</sup> Among these techniques, electrowetting draws most attention due to its high performance, reliability, simplicity, and fast response. Based on the droplet manipulation, one is able to integrate different cumbersome laboratory operations in a microliter liquid, called lab in a drop.<sup>11</sup> Increasing numbers of assays have benefited by this innovation, such as polymerase chain reaction (PCR)<sup>12</sup> and cell sorting.<sup>13</sup> Lately addressable electrowetting has been exploited to extend the technique.<sup>14</sup> Optoelectrowetting (OEW) approach proposed by Chiou *et al.*<sup>15</sup> employs a photoconductor, making “virtual electrodes.” The electrodes are generated dynamically, with projected images, thus realizing multi-droplet and programmable manipulations.

Conventionally, studies put more emphasis on closed configurations (droplets sandwiched in-between two parallel plates). However, integrating additional components or extensibility is seriously limited. An open configuration compensates this deficiency and well-designed combination of open and closed configurations can lead to a complete LoC system as well. In this letter, we propose an addressable open droplet actuation system. This is achieved by integrating open electrowetting<sup>16–19</sup> with a photoconductor resulting in open OEW (o-OEW), as shown in Fig. 1.

A fabrication process regarding the o-OEW chip is briefly described as follow: Firstly, a positive photoresist (Hoechst Celanese, AZ4620) is spun on a 4” glass wafer (Corning, 1737F) and followed by a photolithography. Secondly, 1000-Å titanium (Ti) is deposited on the top of the wafer using e-beam evaporation and then patterned the electrodes by means of lift-off. Subsequently, 450-nm amorphous silicon (a-Si) and 115-nm SiO<sub>2</sub> are deposited using a plasma enhanced chemical vapor deposition (PECVD) system. Here a-Si works as a photoconductor while SiO<sub>2</sub> works as an insulator in the chip. Eventually, a hydrophobic coating of a thickness less than 50 nm is spun on the top surface with 1% diluted Teflon (Dupont, AF1600<sup>®</sup>).

Figure 2 explains the mechanism behind o-OEW. When the circuit loop is located on the dark side of the droplet, the droplet maintains a high contact angle. Otherwise, the major voltage drop occurs in the insulator, causing a wetting force. The liquid curvature change due to the wetted surface decreases the inner pressure which can be estimated from the Young–Laplace equation.<sup>20</sup> Higher pressure on the dark side of the droplet prompts the droplet to move toward the light spot. In principle, the shifting of the impedances between the photoconductor and the insulator determines where the major voltage drop occurs and hence the thickness of each layer should be carefully designed to generate the maximum photoconductivity ratio (i.e., high light-to-dark conductivity ratio).

Compared to the featureless electrode in a closed OEW,<sup>15,21</sup> the key to o-OEW is patterning driving and reference electrodes alternately, such that subcircuit loops are formed when the droplet rolls over them. The interdigitated design aims to increase the contact surface and minimize the discontinuity due to the gap. The minimum droplet size is

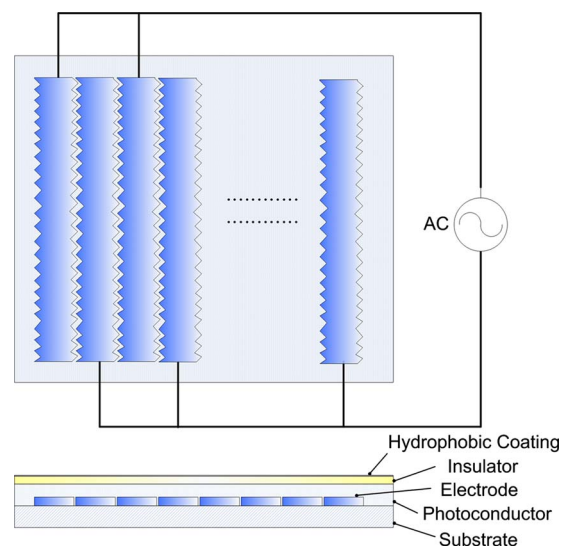


FIG. 1. (Color online) Schematic diagram of the chip layout. The reference and the driving electrodes sit next to each other alternately. The interdigitated edge is used to decrease the discontinuity due to the gap. The materials from the bottom to the top are glass substrate, Ti electrodes, a-Si (photoconductor), SiO<sub>2</sub> (insulator), and Teflon (hydrophobic coating).

<sup>a)</sup>Electronic mail: wereley@purdue.edu.

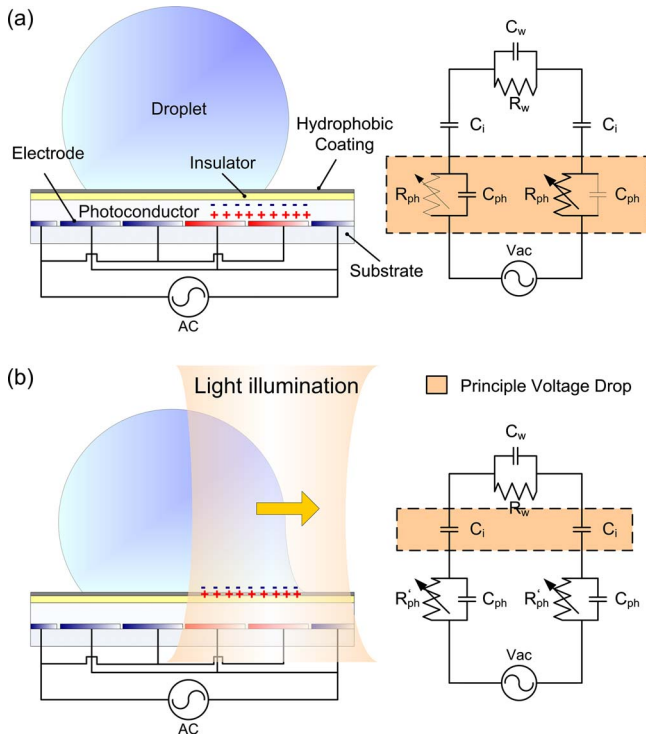


FIG. 2. (Color online) Mechanism of the switching effect for the o-OEW. (a) The liquid droplet maintains a high contact angle and the principle voltage drop falls in the photoconductor in an initial state (without illumination). (b) The impedance of the photoconductor significantly reduces, shifting the voltage drop to the insulator in an excited state (with illumination).

primarily constrained by the electrode width. A controllable droplet should cover at least three electrodes in order to form two different loops on both sides. One side attains a reduced contact angle due to the illumination; the other side maintains a high contact angle in the dark.

For analyzing the droplet actuation in a systematic way, an equivalent circuit for Fig. 2 can be expressed as

$$U_{OEW} = U \left( \frac{\frac{1}{i\omega C_i}}{\frac{2}{i\omega C_i} + \frac{R_w}{1 + i\omega C_w} + \frac{2R_{ph}}{1 + i\omega C_{ph}}} \right), \quad (1)$$

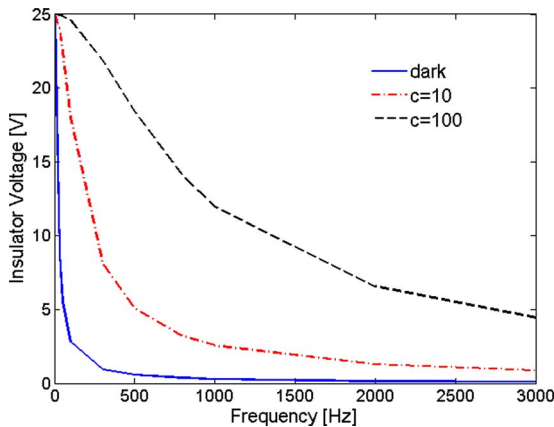


FIG. 3. (Color online) Voltage drop in the insulator vs driving frequency. Notation  $c$  denotes the photoconductivity ratio (light-to-dark conductivity ratio). The optimal operational region yields the maximum photoconductivity ratio. The driving potential was  $50 V_{rms}$  and the empirically operational bandwidth was between 100 and 800 Hz. The frequency out of the range could result in limited or none o-OEW effect.

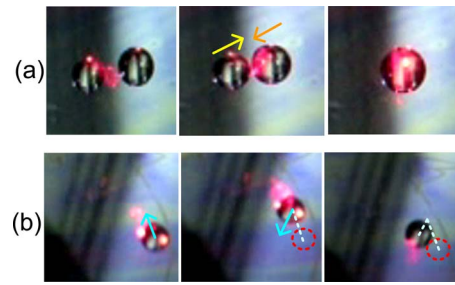


FIG. 4. (Color online) Basic droplet manipulations using an o-OEW device. The driving voltage was  $42 V_{rms}$  at 500 Hz. (a) The laser spot is placed in the middle of the two droplets, causing both droplets to wet the illuminated surface and then merge together. (b) Transporting is demonstrated. In the image set from left to right, the droplet initially moves to the upper left (Second image) and then to the lower left (third image). The simple maneuvering proves the potential of free droplet operations on a surface.

where  $U$  is the driving potential,  $C_i$ ,  $C_w$ , and  $C_{ph}$  are the capacitances of the insulator, the droplet, and the photoconductor, respectively,  $R_w$ , and  $R_{ph}$  are the resistances of the droplet and the photoconductor, respectively, and  $\omega$  denotes the driving angular frequency. The hydrophobic coating (DuPont, Teflon AF1600) used to maintain a high contact angle ( $\sim 118^\circ$ ) is usually relatively thin, thus being excluded in the calculation for simplicity.

Relationship between the voltage drop across the insulator and the driving frequency is exhibited in Fig. 3. The objective is to seek a frequency which can provide the maximum photoconductivity ratio. The voltage drop declines rapidly as the frequency increases and no significant voltage difference between the dark and bright is observed at low frequency ( $\ll 100$  Hz), resulting in merely a narrow bandwidth available for manipulation. Compared to experimental observations ( $10 < c < 100$ ), the optimal bandwidth based on the current setup falls between 100 and 800 Hz. An increase in light intensity is likely to enhance the photoconductivity ratio.

An evaluation of contact angle measurement was conducted. A potential of  $37 V_{rms}$  at 100 Hz was applied on a liquid droplet (water). The illumination laser source (3 mW) was  $15 \text{ mW/cm}^2$  at 670 nm, and it was used for both actuation and contact angle measurements. A contact angle reduction of  $24^\circ$  was experimentally observed while reported hysteresis angle on the same hydrophobic surface is  $7^\circ\text{--}9^\circ$ .<sup>22</sup> More information associated with the experimental and theoretical analyses can be obtained from the works of Chiou *et al.*<sup>23</sup> and Inui.<sup>24</sup>

Figure 4 demonstrates fluid transport utilizing o-OEW. The movement of the droplet in a triangle path [Fig. 4(b)] manifests free movement in all directions on the surface. Translational speeds up to 3.6 mm/s were experimentally measured. The use of titanium (Ti) makes it necessary for the laser/steering beam to come in from the top. However, the metal can be replaced by a transparent conductive material, such as indium tin oxide, thus enabling the laser beam to come in from the bottom (flat side of the droplet). Furthermore, a test without potential supply was also conducted to observe the possible actuation resulting from Marangoni effect. No displacement was measured under such circumstances and the temperature increase due to the laser heating was too tiny ( $< 0.1^\circ\text{C}$ ) to be measured.

Overall this paper demonstrates a unique technique of droplet actuation using an open configuration OEW with coplanar electrodes and a photoconductor. The results amend the deficiency of the current OEW, leading to a more complete programmable LoC system.

- <sup>1</sup>M. G. Pollack, R. B. Fair, and A. D. Shenderov, *Appl. Phys. Lett.* **77**, 1725 (2000).
- <sup>2</sup>J. Zeng and T. Korsmeyer, *Lab Chip* **4**, 265 (2004).
- <sup>3</sup>S. K. Cho, H. Moon, and C. J. Kim, *J. Microelectromech. Syst.* **12**, 70 (2003).
- <sup>4</sup>S. Y. Teh, R. Lin, L. H. Hung, and A. P. Lee, *Lab Chip* **8**, 198 (2008).
- <sup>5</sup>O. D. Velev, B. G. Prevo, and K. H. Bhatt, *Nature (London)* **426**, 515 (2003).
- <sup>6</sup>K. T. Kotz, Y. Gu, and G. W. Faris, *J. Am. Chem. Soc.* **127**, 5736 (2005).
- <sup>7</sup>R. D. Sun, A. Nakajima, A. Fujishima, T. Watanabe, and K. Hashimoto, *J. Phys. Chem. B* **105**, 1984 (2001).
- <sup>8</sup>D. Beyssen, L. L. Brizouala, O. Elmazriaa, and P. Alnot, *Sens. Actuators B* **118**, 380 (2006).
- <sup>9</sup>K. L. Wang, T. B. Jones, and A. Raisanen, *J. Micromech. Microeng.* **17**, 76 (2007).
- <sup>10</sup>H. Moona, S. K. Cho, R. L. Garrell, and C. J. Kim, *J. Appl. Phys.* **92**, 4080 (2002).
- <sup>11</sup>A. Sukhanova, Y. Volkov, A. L. Rogach, A. V. Baranov, A. S. Sussha, D. Klinov, V. Oleinikov, J. H. M. Cohen, and I. Nabiev, *Nanotechnology* **18**, 185602 (2007).
- <sup>12</sup>Y. H. Chang, G. B. Lee, F. C. Huang, Y. Y. Chen, and J. L. Lin, *Biomed. Microdevices* **8**, 215 (2006).
- <sup>13</sup>S. K. Cho and C. J. Kim, Proceedings of the 16th IEEE Annual International Conference on Micro Electro Mechanical Systems, MEMS '03, Kyoto, Japan, 19–23 January 2003, pp. 686–689.
- <sup>14</sup>S. K. Fan, C. Hashi, and C. J. Kim, Proceedings of the 16th IEEE Annual International Conference on Micro Electro Mechanical Systems, MEMS '03, Kyoto, Japan, 19–23 January 2003, pp. 694–697.
- <sup>15</sup>P. Y. Chiou, H. Moon, H. Toshiyoshi, C. J. Kim, and M. C. Wu, *Sens. Actuators, A* **104**, 222 (2003).
- <sup>16</sup>C. G. Cooney, C. Yi. Chen, M. R. Emerling, A. Nadim, and J. D. Sterling, *Microfluid. Nanofluid.* **2**, 435 (2006).
- <sup>17</sup>U. C. Yi and C. J. Kim, *J. Micromech. Microeng.* **16**, 2053 (2006).
- <sup>18</sup>A. Torkkeli, VTT PUBLICATIONS, Vantaa, Finland (2003).
- <sup>19</sup>J. Wu, R. Yue, X. Zeng, M. Kang, Z. Wang, and L. Liu, Proceedings of the first IEEE International Conference on Nano/Micro Engineered and Molecular Systems, NEMS '06, Zhuhai, China, 18–21 January 2006, pp. 1152–1155.
- <sup>20</sup>H. D. Young, *Physics*, 8th ed. (Addison-Wesley, Reading, MA, 1992).
- <sup>21</sup>P. Y. Chiou, A. T. Ohta, and M. C. Wu, *Nature (London)* **436**, 370 (2005).
- <sup>22</sup>J. Berthier, P. Dubois, P. Clementz, P. Clause, C. Peponnet, and Y. Fouille, *Sens. Actuators, A* **134**, 471 (2007).
- <sup>23</sup>P. Y. Chiou, Z. Chang, and M. C. Wu, *J. Microelectromech. Syst.* **17**, 133 (2008).
- <sup>24</sup>N. Inui, *Sens. Actuators, A* **140**, 123 (2007).